Electronic Supplementary Material (ESI) for Physical Chemistry Chemical Physics.

Supporting Information

Structural engineering brings new electronic properties to Janus ZrSSe and HfSSe monolayers

Xinxin Wang, Shuhui Zhang, Yuanyuan Wang, Shiqiang Yu, Baibiao Huang, Ying Dai,* and Wei Wei*

School of Physics, State Key Laboratory of Crystal Materials, Shandong University, Jinan 250100, China

* Corresponding authors: daiy60@sdu.edu.cn (Y. Dai), weiw@sdu.edu.cn (W. Wei)

Table S1 Optimized interlayer distance (d), binding energy (E_b) and band gap (E_g) of the out-of-plane vdW heterostructures of T-ZrSSe/T-HfSSe.

	AA	AA'	AB	AB'	A'B
d (Å)	2.90	3.55	3.03	3.57	2.97
E_b (eV)	–1.98	–1.89	–1.96	–1.93	–2.01
E_g (eV)	0.68	0.65	0.61	0.53	0.55

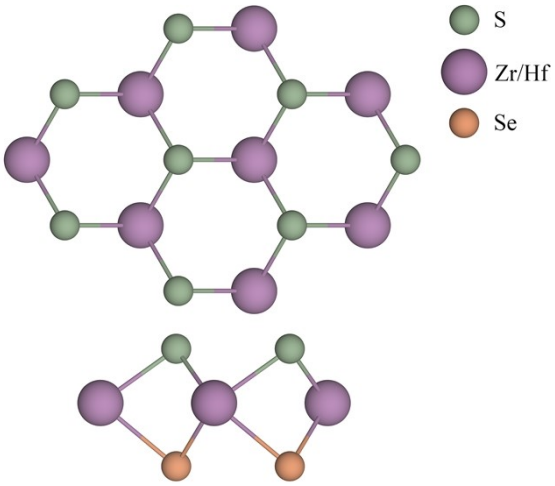

Figure S1. Top and side views of atomic structure for H-ZrSSe and H-HfSSe.

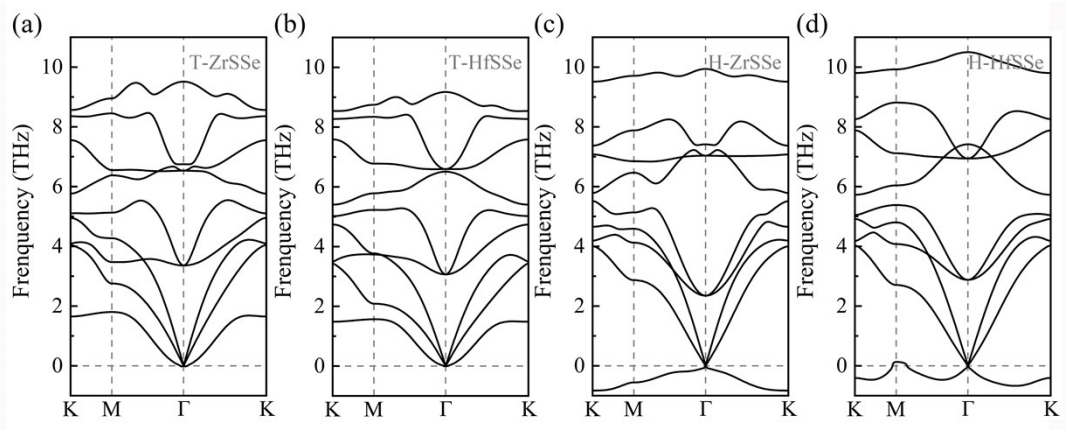

Figure S2. Phonon spectrum of (a) T-ZrSSe, (b) T-HfSSe, (c) H-ZrSSe and (d) H-HfSSe.

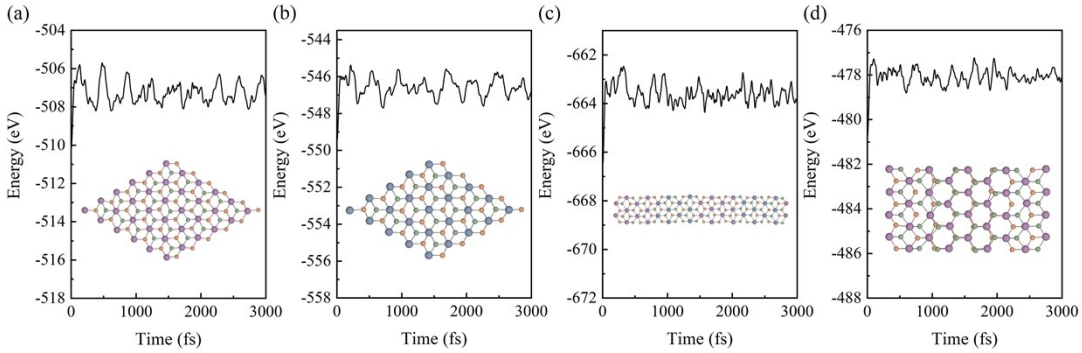

Figure S3. AIMD simulation results for (a) T-ZrSSe, (b) T-HfSSe, (c) in-plane heterostructure, (d) electronic heterostructure with 1D phase boundary, at 300 K lasting for 3 ps. Insets are snapshots of the final structures.

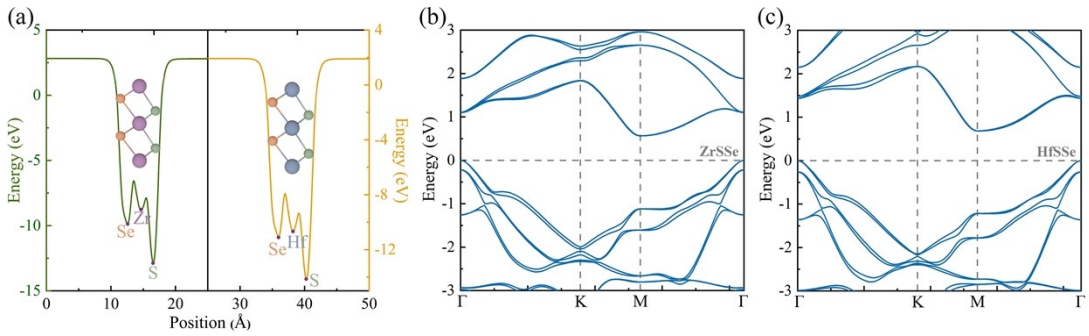

Figure S4. (a) Planner-averaged electrostatic potential energy for (a) T-ZrSSe (left) and T-HfSSe (right). Band structure taking SOC into account for (b) T-ZrSSe, and (c) T-HfSSe monolayer, the Fermi level is set to zero.

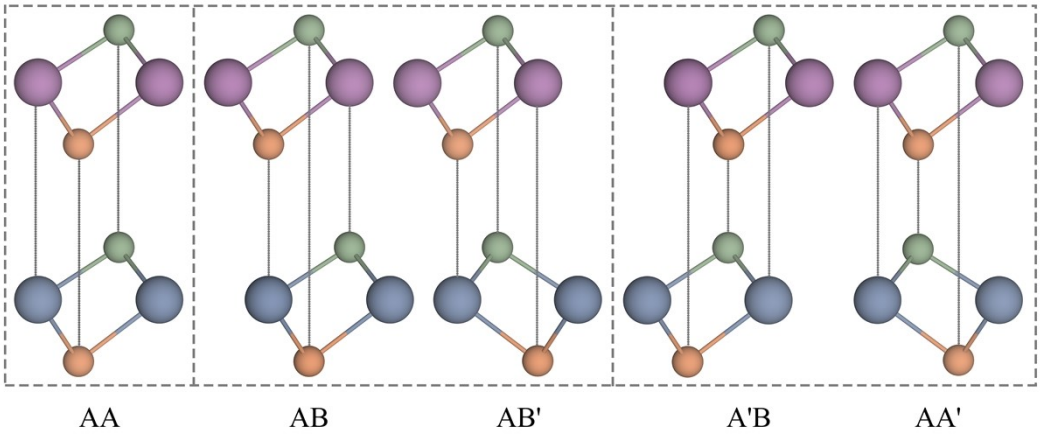

Figure S5. Stacking patterns of high-symmetry for out-of-plane vdW heterostructures composed of T-ZrSSe and T-HfSSe.

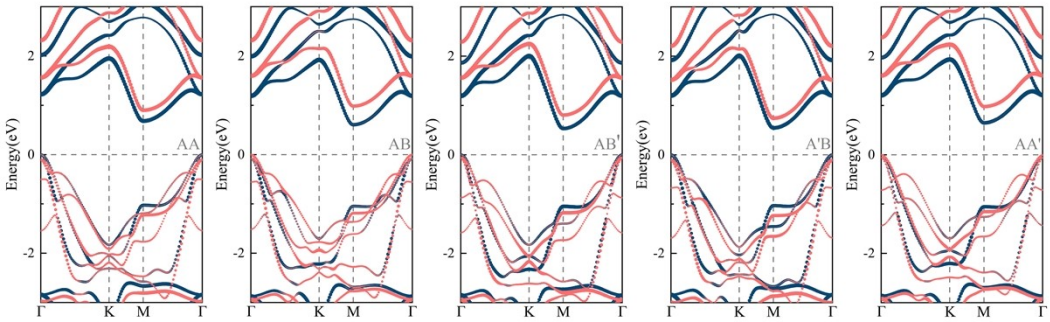

Figure S6. Projected band strucure for out-of-plane vdW heterostructure composed of T-ZrSSe and T-HfSSe, contributions from T-ZrSSe and T-HfSSe are distinguished by navy-blue and orange dots, respectively. The Fermi level is set to zero.

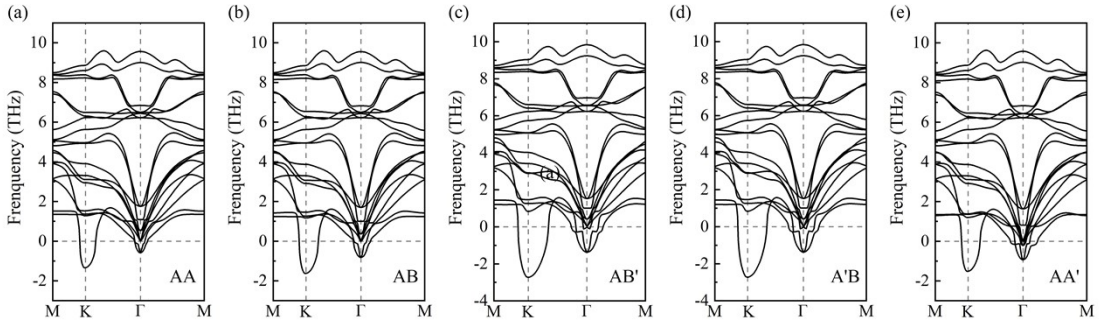

Figure S7. Phonon spectrum for out-of-plane heterostructures composed of T-ZrSSe and T-HfSSe of different stacking order: (a) AA, (b) AB, (c) AB', (d) A'B, and (e) AA'.

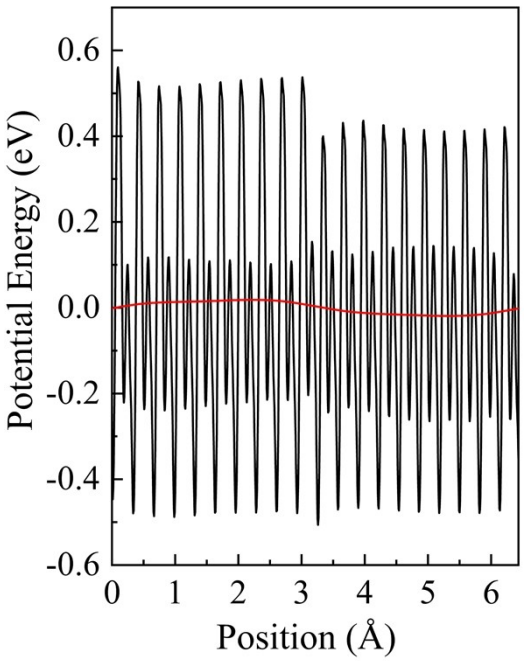

Figure S8. Planar-averaged electrostatic potential along the direction perpendicular to the interface for in-plane heterostructures of T-ZrSSe and T-HfSSe (n = 10), and the macroscopic-average of the electrostatic potential (red line) is also shown.

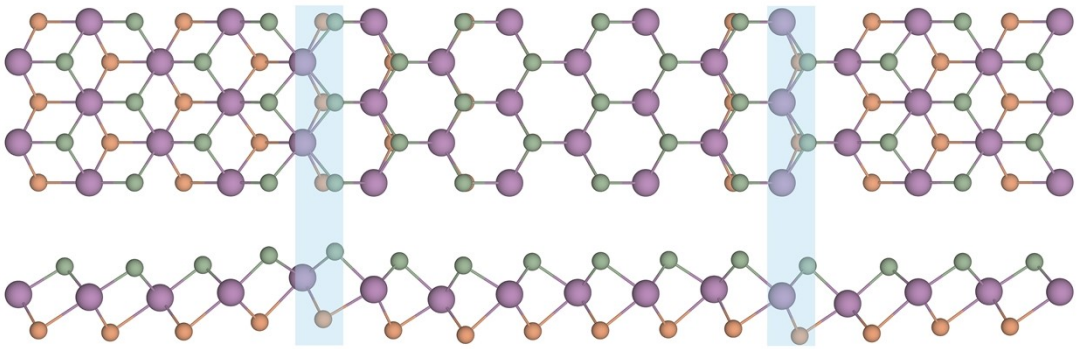

Figure S9. Relaxed structure of the electronic heterostructure between T- and H-ZrSSe with the 1D phase boundary along the zigzag direction.

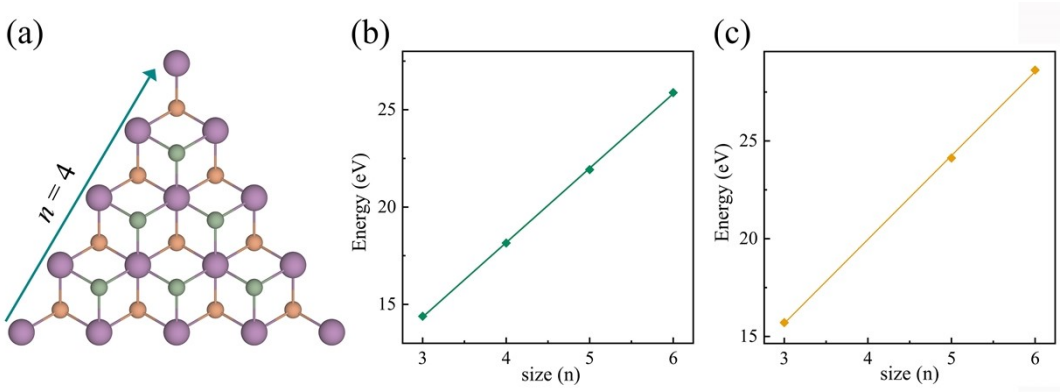

Figure S10. (a) Triangular structure used to calculate the edge energy σ of type-I GBs, where n denotes the number of Se atoms on each edge. Energy of the triangular structure of (b) ZrSSe and (c) HfSSe as a function of n. In (b) and (c), thus, the slope corresponds to the edge energy σ.

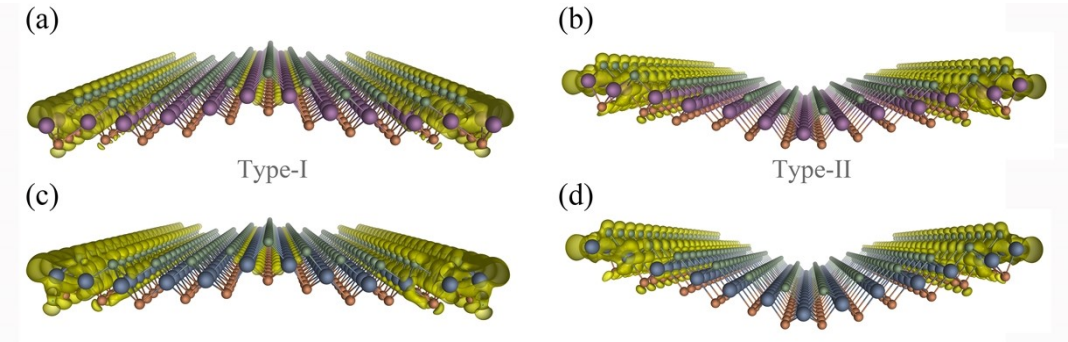

Figure S11. Charge density distribution of the states near the Fermi level for GBs of (a) type-I nad (b) type-II in T-ZrSSe, and of (c) type-I and (d) type-II in T-HfSSe.